Notes

High-Resolution Solid-State NMR of B-Type Amylose

C. Rondeau-Mouro,*,† G. Veronese,‡ and A. Buleon§

UR BIA-INRA, Laboratoire de RMN, Plate-forme-BIBS, Rue de la Géraudière, BP 71627, 44316 Nantes Cedex 3, France, INSA DGBA, UMR INRA 792, UMR CNRS 5504, 135 avenue de Rangueil, 31077 Toulouse Cedex 4, France, and UR BIA-INRA, Equipe Structures des assemblages semi-cristallins, Rue de la Géraudière, BP 71627, 44316 Nantes Cedex 3, France

Received April 4, 2006
Revised Manuscript Received June 7, 2006

Introduction

Starch, the major energy reserve of higher plants, is a mixture of two main components: amylose, a linear or slightly branched (1,4)-α-D-glucan, and amylopectin, a highly branched macromolecule consisting of (1,4)-α-D-glucan short chains linked through α(1,6) linkages.[1] All starches are biosynthesized as semicrystalline granules in which these two polysaccharides are densely packed with little water included. The crystallinity (about 20−45%[2,3]) and the polymorphism of starch, as revealed by X-ray diffraction analysis, have been recognized for a long time, and three main types (A, B, and V) have been reported.[4−8] On the contrary to A and B polymorphs, the V polymorph is rarely detected as a crystalline material in native starches[3,9] but essentially results from the complexation of amylose with compounds such as iodine, alcohols, or lipids. Amylose can also recrystallize from solutions into A- or B-type as lamellar,[10,11] fibrillar,[12,13] or spherulitic crystals, as well as polycrystalline powders.[11,14] The resulting morphology and allomorphic type depend on temperature of crystallization, concentration, solvent, and degree of polymerization (DP).[10,15−17] A general rule is that long chains and low recrystallization temperature favor B-type, whereas high concentration, high temperature, and short chains are known to induce A-type crystallization**.** This ability has been used to determine the three-dimensional structures of these different polymorphs. A double helical conformation is assumed for amylose chains in A and B forms.[12,13,18−20] In the A-type structure, left-handed parallel-stranded double helices are packed in the monoclinic space group B2.[18] In the B-type structure, the double helices are packed in a hexagonal unit cell with the $P6_1$ space group.[19,20]

Solid-state NMR has proven to be a powerful tool for assessing the conformation and the crystalline structure of starchy substrates.[21−26] The chemical shift of the anomeric C1 carbon resonance is directly related to dihedral angles along the glycosidic linkage, while crystallographic constraints may induce the splitting of the peak.[21−24,27] Therefore, the three distinct crystalline forms of starch can be distinguished by the ^{13}C NMR characteristics of the anomeric C1 carbon signal. The C1 peak of the A-type structure displays a cluster of three signals, while for the B-type structure, a multiplicity of two peaks is observed. In the case of a complex with a small molecule (lipid, aromatic, or alcohol, for example), the C1 signal shows a single resonance characteristic from the V conformation.[24,28−30] In all these hydrated structures, the ordering effect of water is known to reduce the bandwidth in cross-polarization magic angle spinning (CP-MAS) spectra.[27,31−33] Nevertheless, on starchy samples, the presence of amorphous regions and the low abundance of ^{13}C in the samples render the spectra recording times very long and high-resolution experiments very difficult. Such experiments were carried out on cellulose and chitin, and it allowed the complete assignment of the CP-MAS spectra.[34−37]

More recently, amylose particles with exceptionally high B-type crystallinity and original axialitic or spherulitic structure were obtained by in vitro synthesis of amylose using the amylosucrase enzyme from *Neisseria polysaccharea*.[38] From sucrose as the sole substrate, this enzyme catalyzes the synthesis of a linear (1,4)-α-D-glucan (amylose-like polymer) and releases fructose.[39] This study describes its use for the preparation of ^{13}C-labeled amylose axialitic crystals and their study by high-resolution solid-state NMR. The assignment of the complete B-type amylose spectrum and correlations between $^{13}C-^{13}C$ distances and the atomic positions in the three-dimensional structure of B-type are discussed.

Experimental Section

Material. *Labeled Sucrose.* ^{13}C-labeled (99%) D-sucrose was obtained from Sigma-Aldrich (France).

Plasmid and Bacterial Strain. The gene encoding amylosucrase was isolated from Neisseria polysaccharea ATCC 43768 chromosomal DNA. The pGST-AS encoding glutathione-S-transferase fused to amylosucrase[40] was used to express the fusion gene. *Escherichia coli* strain BL21 was used as the host of pGST-AS encoding fusion protein.

Method. *Enzyme Extraction and Purification.* Gene expression, recombinant cell growth, enzyme extraction, and purification were carried out as previously described.[40] Amylosucrase was purified by affinity chromatography between the glutathione-S-transferase/amylosucrase fusion protein (molecular weight 96 kDa) and glutathione−Sepharose 4B (Amersham Biosciences). Since pure fusion protein displays the same catalytic properties as pure amylosucrase (data not shown), the glutathione-S-transferase tag (26 kDa) was not removed.

In Vitro Synthesis of Amylose. Reaction was performed at 30 °C, in 50 mM Tris-HCl buffer, pH 7.0, containing 600 mM ^{13}C-labeled sucrose and 275 mg·L^{-1} pure glutathione-S-transferase/amylosucrase fusion protein. The reaction medium was stirred for 28 h. At the end of the reaction, the medium was heated 5 min at 90 °C to stop the enzyme action, and the precipitate was separated by centrifugation (10 min, 10 000*g*). The precipitate was washed three times using 1 volume of water and finally once using 1 volume of water containing 0.02% (w/v) NaN_3.

X-ray Diffraction. X-ray diffraction was performed after adjustment of the water content of the washed precipitate by water desorption at 90% of relative humidity (RH) for 10 days under partial vacuum in the presence of a saturated baryum chloride solution. The sample (20 mg) was sealed between two tape foils to prevent any significant change in water content during the measurement. Diffraction diagrams were

* Corresponding author. rondeau@nantes.inra.fr, telephone number 33-(0)2-40-67-50-50, fax number 33-(0)2-40-67-50-84.
† UR BIA-INRA, Laboratoire de RMN.
‡ INSA DGBA.
§ UR BIA-INRA, Equipe Structures des assemblages semi-cristallins.

10.1021/bm060330x CCC: $33.50
Published on Web 07/19/2006

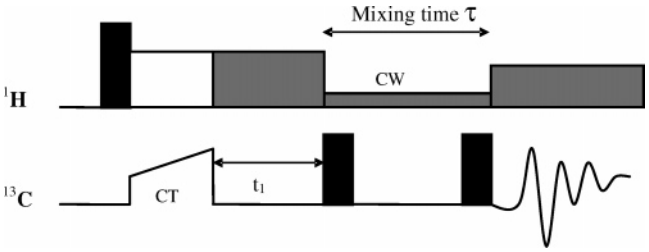

Figure 1. Pulse sequence for the DARR experiment. After cross-polarization using a ramped pulse on the ^{13}C channel (contact time, CT), magnetization evolves during t_1 and is placed along the *z*-axis with a 90° pulse. Then, the mixing period τ occurs with a low power ^{1}H recoupling pulse (CW) before detection with a high-power level of ^{1}H decoupling.

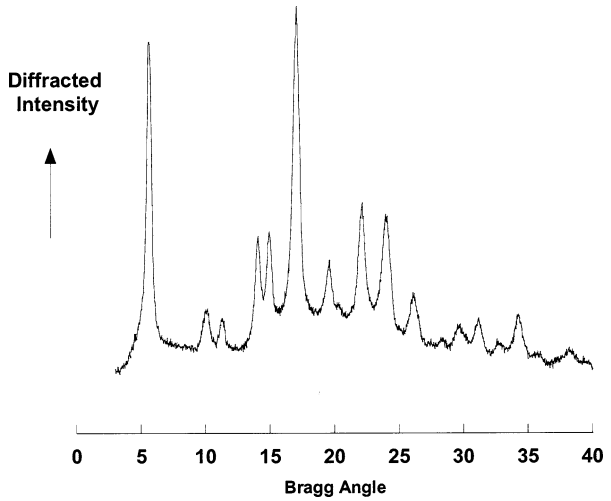

Figure 2. X-ray diffraction diagram of the ^{13}C-labeled B-type axialitic amylose.

recorded using an INEL (Artenay, France) spectrometer working at 40 kV and 30 mA operating in the Debye−Scherrer transmission mode. The X-ray radiation Cu Kα_1 (λ = 0.154 05 nm) was selected with a quartz monochromator. Diffraction diagrams were recorded during 2 h exposure periods, with a curve position-sensitive detector (INEL CPS 120). Relative crystallinity was determined using the method initially developed by Wakelin et al.[41] for cellulose. Spherulitic B-type recrystallized amylose was used as the crystalline standard, after scaled subtraction of an experimental amorphous curve in order to get null intensity in the regions without diffraction peaks. Dry extruded potato starch was used as the amorphous standard. All diagrams (sample and standards) were normalized at the same integrated scattering between $2\theta = 3°$ and 40° before their use for the calculation of the crystallinity.

Measurement of the Carbon−Carbon Distances in the B-Type Structure Model. The coordinates of the asymmetric unit were taken from the paper of Imberty and Perez.[19] The packing of double helices in the crystal was generated from the space group and the unit cell parameters using the Insight molecular modeling package (Accelrys, San Diego, U.S.A.). The different distances between the carbons belonging either to the same double helix or to two neighboring double helices were measured using the same software. All the distances smaller than 1 nm were considered.

NMR. NMR experiments were performed on a Bruker DMX-400 spectrometer operating at a ^{13}C frequency of 100.62 MHz and equipped with a double-resonance H/X CP-MAS 4-mm probe for CP-MAS solid-state experiments. The MAS rate was fixed at 10 kHz, and each experiment was recorded at ambient temperature (294 ± 1 K). The cross-polarization pulse sequence used a 3.75-μs 90° proton pulse, a 1-ms contact time at 66.7 kHz, and a 10-s recycle time for an acquisition time of 17 ms during which dipolar decoupling (TPPM) was applied. A typical number of 8 scans were acquired for the CP-MAS spectrum. Chemical shifts were calibrated with external glycin, assigning the carbonyl carbon at 176.03 ppm. Two-dimensional refocused INADEQUATE spectrum of amylose was recorded with a total of 256 t_1

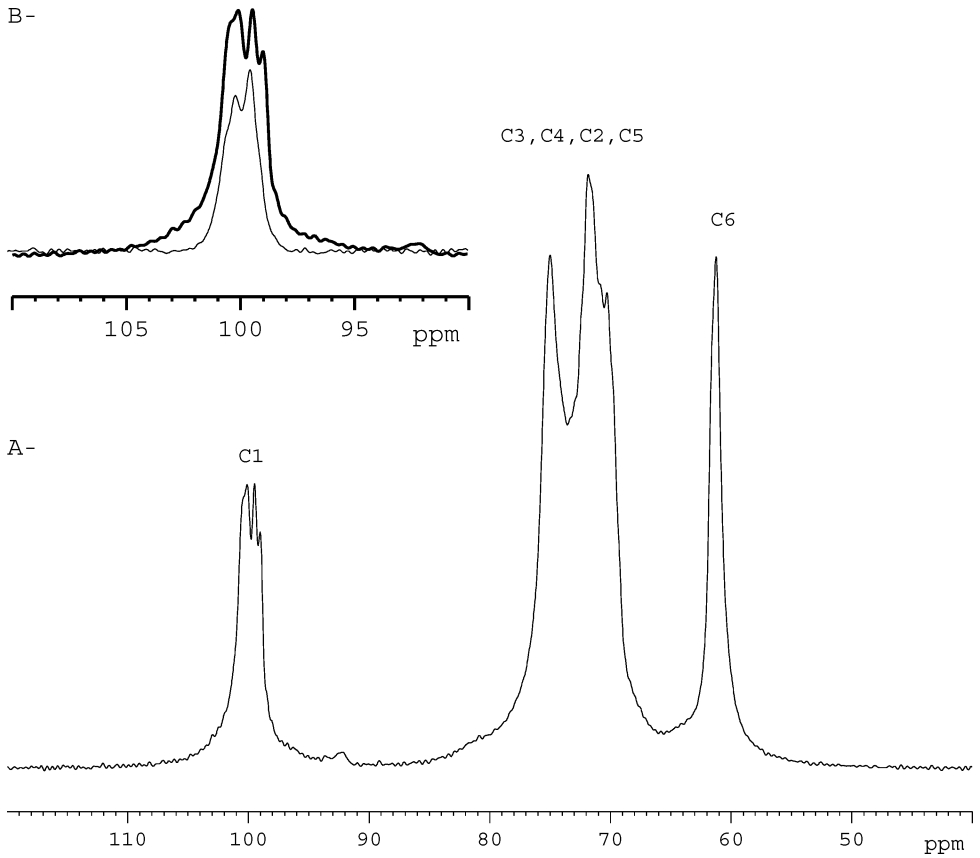

Figure 3. ^{13}C CP-MAS NMR spectra of ^{13}C-labeled B-type axialitic amylose (A), and superimposition of the C1 resonance of ^{13}C-labeled B-type axialitic amylose acquired using CP-MAS (bold line) and the IPAP sequence for C1−C2 scalar decoupling (thin line) (B).

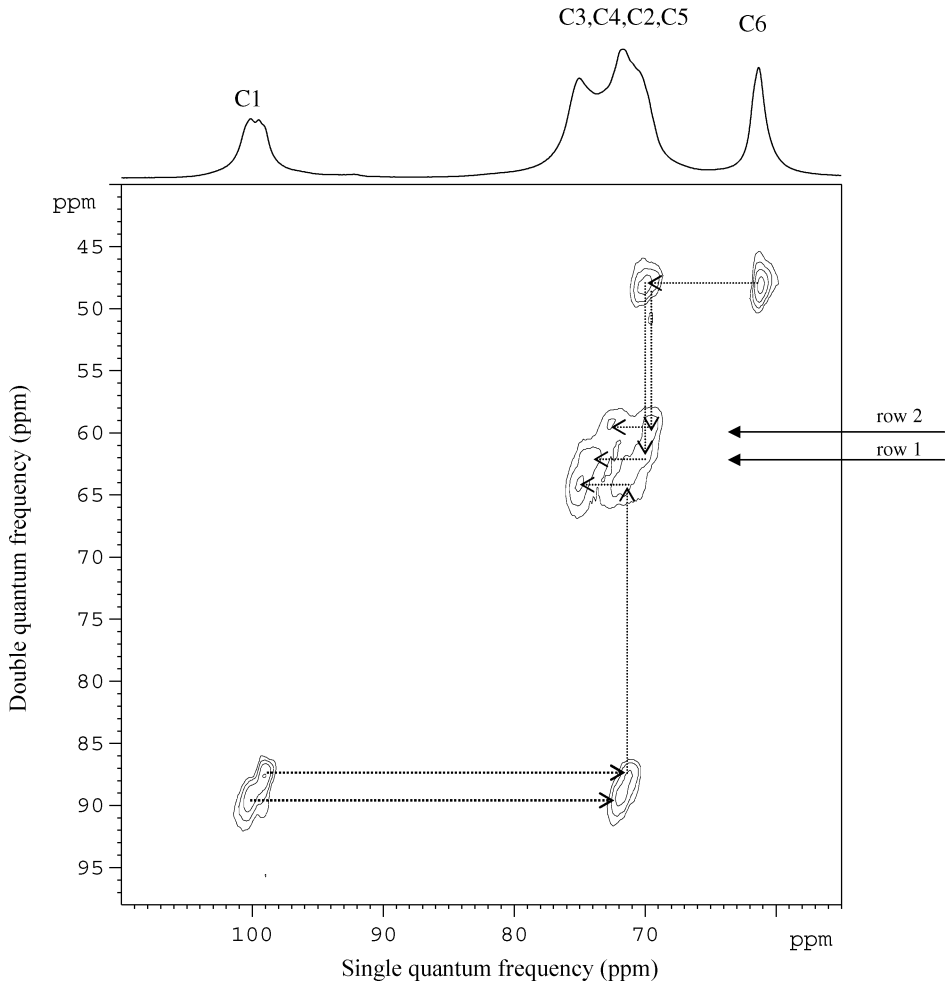

Figure 4. Refocused INADEQUATE of ^{13}C-labeled B-type axialitic amylose.

increments of 256 scans.[34] The cross-polarization parameters in the sequence were chosen as above, and the delay τ during which the J couplings evolve was set to 4 ms. Quadrature detection was achieved using the TPPI method.[42] The homonuclear scalar coupling between the amylose carbons C1 and C2 was removed using the IPAP spin-state selection filter[43] in the CP-MAS sequence. For optimal performance of the IPAP filter, the delay τ was adjusted to 8 ms ($J_{CC} = 62.5$ Hz), and the durations of the soft pulses were calibrated to 2 ms. The DARR sequence[44] used a low-power proton "recoupling" pulse of 10 kHz during the mixing period τ, corresponding to the $n = 1$ rotational resonance condition (see sequence in Figure 1). The rotational resonance (R^2) technique is commonly used to recouple homonuclear spin pairs in rotating solids.[45−47] The R^2 condition was achieved by matching the chemical shift difference (in Hz) between a pair of selected lines in the carbon spectrum with a multiple of the sample spinning frequency ($\Delta = n\nu_R$). Rotational resonance coupled with the DARR experiment has been applied between each glycosidic carbon of amylose except for C4 showing no isolated resonance in the 1D spectrum. The buildup rates k of the signals' evolution during the mixing time were determined by fitting the measured data to the following single-exponential function:

$$\frac{S_{(\tau)}}{S_0} = \eta[1 - \exp^{(k,\tau)}]$$

using η and k as fitting parameters, while $S_{(\tau)}$ represents the signal intensities at the mixing time delay τ and S_0 the signal intensities for no mixing period. Correlations between carbon distances estimated by molecular modeling and the buildup rates k was achieved under EXCEL (Microsoft).

Results and Discussion

NMR studies of solid-state biopolymers can be a true challenge because of important dipolar interactions inducing large and sometimes superimposed signals. These anisotropic interactions render the analysis of solid biopolymers by ^{1}H NMR very difficult. Nevertheless, their characterization using solid-state ^{13}C NMR has shown that important structural and dynamic information could be obtained using CP-MAS experiments. On the other hand, NMR investigations of starch and its constituents yield spectra with poor resolution demanding long acquisition times because of their weak crystallinity and their low natural ^{13}C content. Moreover, while solid-state NMR is considered a noninvasive technique of high importance in order to describe the different crystal structures and helical conformations present in amylose and starch polymorphs, it was not possible up to now to definitely assign their complete spectra or to perform some high-resolution NMR experiments. To circumvent to these difficulties, an in vitro enzymatic synthesis of highly crystalline amylose was performed using labeled ^{13}C sucrose. The average degree of polymerization ($\overline{DP}$) in the precipitated product was 35 with a polydispersity of 2.3. The water content resulting from storage at 90% of relative humidity (RH) for 10 days and used for X-ray and NMR experiments was 21% (dry basis).[38]

Figure 2 shows the X-ray diffraction diagram of the precipitate formed during the enzymatic synthesis of ^{13}C-labeled amylose. The diagram is characteristic of a pure B-type crystal structure similar to that resulting from amylose or amylopectin recrystallization in water, with main diffraction peaks appearing

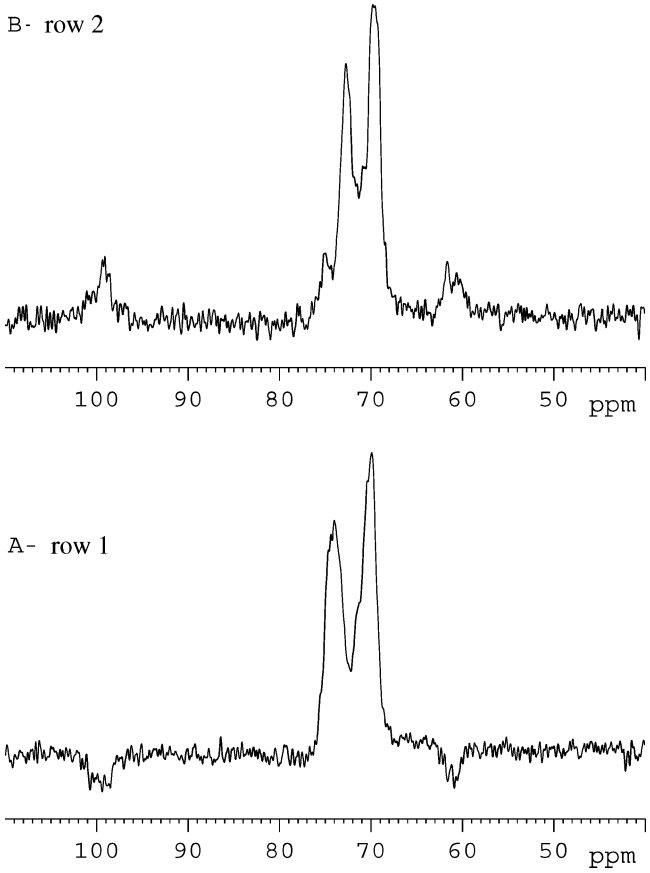

Figure 5. Rows extracted from the refocused INADEQUATE spectrum showing correlations between the carbon C5 at 70.2 ppm and the C4 at 74.3 ppm (row 1 in Figure 4A) and between the other C5 signal at 69.8 ppm with the second C4 signal at 72.6 ppm (row 2 in Figure 4B).

at $2\theta = 5.6°$, 15°, 17°, 22°, and 24°. The crystallinity was found to be 90% ± 3%, which is exceptionally high for amylose and in agreement with the value found for unlabeled amylose prepared in the same conditions.[38] In that case, this crystallinity has been related to the formation of B-type axialitic particles during amylose synthesis by amylosucrase.[38]

Such a ^{13}C-labeled amylose substrate (with a very high crystallinity) has never been prepared before and allowed to record well-resolved NMR spectra in a very short time. Figure 3A shows the CP-MAS spectrum of this ^{13}C enriched amylose, recorded in less than 2 min instead of several hours in the case of nonenriched amylose. The spectrum feature is characteristic of a polymer of glucose with three distinguishable regions, one for the anomeric C1 carbon around 100 ppm, the other around 72 ppm for, presumably, the C2, C3, C4, and C5 carbons, and the last peak at 60 ppm assigned to C6. The C1 signal shows a fourfold resonance instead of the usual twofold multiplicity observed for B-type amylose, related to the symmetry of the double helix.[21−24,27] In the B-type crystalline packing, the six-fold strand of the double helix consists of three maltose repeats, and therefore, two different (1,4) glycosidic linkages, respectively, within and between the maltose repeats, are present. The splitting in four resonances observed here was induced by homonuclear scalar coupling between directly bound C1 and C2 carbons, detectable because of the 100% ^{13}C enrichment. This was demonstrated by removing the contribution of carbon *J*-couplings using a spin-state selection filter in the classical CP-MAS sequence. The filter used to eliminate the *J*-coupling between the two spins C1 and C2 was based on the application

Table 1. Carbon Assignments of the Crystalline ^{13}C-Labeled B-Type Axialitic Amylase

carbon	C1	C2	C3	C4	C5	C6
δ (ppm)	100.2	72.1	75.1	74.3	70.2	61.3
	99.3	71.3		72.6	69.8	

of two 180° selective pulses on the C2 spin, at the middle of the scalar coupling evolutions of the C1 spin.[43] The resulting spectrum is shown in the inset (B) of the Figure 3. It was the first time that such an experiment, called IPAP for in-phase−anti-phase, was used on such a macromolecule. The IPAP filter can also be considered a tool to confirm the assignment of the C2 resonance. Indeed, the homonuclear C1−C2 scalar coupling was removed by applying a π-pulse on the C2 resonance at the middle of each $\tau/2$ evolution period of the C1 spin. The knowledge of the C2 frequency was necessary to realize the decoupling.

A complete assignment of the ^{13}C CP-MAS spectrum was also possible, thanks to the use of high-resolution solid-state NMR sequences applicable to enriched ^{13}C starchy substrates. Final assignment of the resonances centered at 72 ppm was achieved by recording the refocused INADEQUATE spectrum presented in Figure 4. This experiment allowed the identification of the directly linked carbons through their common frequency in the double-quantum dimension (peaks on the same horizontal line called row in 2D-NMR spectroscopy). If one carbon is connected to more than one other carbon, the corresponding peak connection is found at the same chemical shift in the single-quantum dimension (peaks on the same vertical line called column in 2D-NMR spectroscopy) but at another double-quantum frequency. According to these rules, the anomeric carbon C1 which displays two resonances at 100.2 and 99.3 ppm is correlated with the two resonances of C2 carbon at 72.1 and 71.3 ppm (see and follow the arrows on Figure 4). These C2 resonances have a second clear correlation in the double-quantum frequency domain which leads to the identification of a C3 resonance at 75.1 ppm. The methylene C6 carbon at 61.3 ppm is connected with C5 at 70.2 ppm, which displays a net correlation with C4 at 74.3 ppm (see row 1 on Figure 4 corresponding to the Figure 5A). This last chemical shift is close to the assignment already proposed for the crystalline C4 carbon around 75 ppm in several studies.[31,48,49] Another correlation is obvious between a signal at 69.8 ppm with a resonance at 72.6 ppm (see row 2 on Figure 4 corresponding to the Figure 5B). These resonances are assigned respectively to C5 and C4, the second signals of the C5 and C4 doublets. Table 1 clearly resumes these assignments.

Dipolar couplings between nuclei are directly related to their spatial proximity. NMR methods using MAS and radio fre-

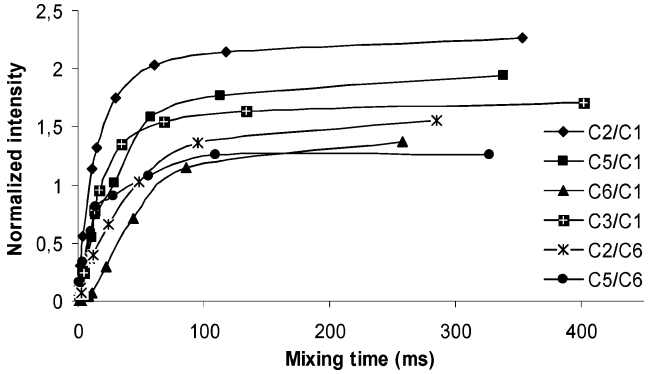

Figure 6. Buildup curves of 2D spectra cross-peak intensity as a function of the mixing time of the DARR experiment.

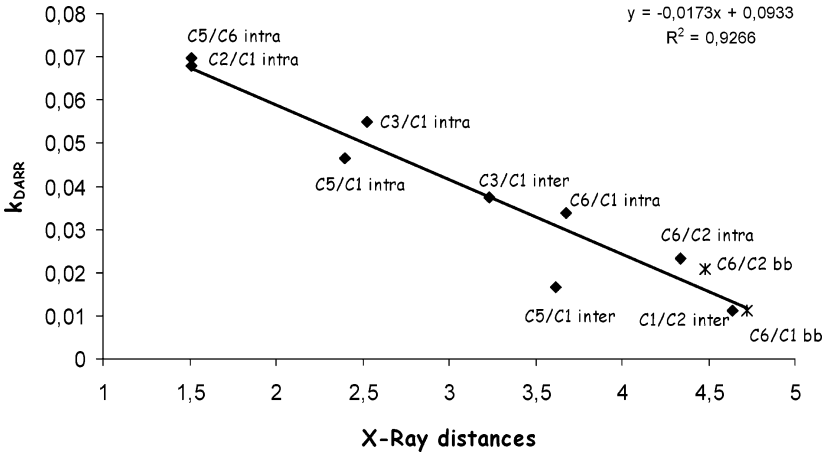

Figure 7. Correlations between the DARR buildup rates and C−C distances measured on the tridimensional model proposed by Imberty and Perez.[19] "intra" designates carbon distances inside the same glycosidic cycle, "inter" refers to carbon distances between two consecutive glycosidic cycles, and "bb" (× symbol) represents carbon distances between two glycosidic cycles in different double helices.

quency pulse sequences for measuring dipolar interactions have been developed since 1988 with the study of the rotational resonance effect in solids.[50] A wide range of sequences has been proposed over the past years in order to improve the efficiency of the dipolar recoupling by reducing artifacts from other interactions and from pulse imperfections (see references in Baldus[51]). One of these, the dipolar assisted rotational resonance sequence (DARR) has been shown to be efficient for rather long-range $^{13}C-^{13}C$ distances even in the presence of strong couplings from directly bound carbons.[44] Moreover, this sequence seems to be less sensitive to radio frequency inhomogeneity than the widely used RFDR experiment (radio frequency driven recoupling). A first application of the DARR sequence on the ^{13}C-labeled amylose is illustrated on Figure 6 showing the buildup curves of 2D spectra cross-peak intensity as a function of the mixing time of the experiment illustrated in Figure 1. It should be noted that the cross-peak intensities are influenced by several factors, including homogeneous $^{1}H-^{1}H$ dipolar interactions, that increase the DARR transfer efficiency and make very difficult the simulation of the C−C distances. However, Takegoshi et al.[52] have demonstrated that it is possible to correlate the cross-peak buildups with internuclear distances. Fitting of the buildup curves using a single-exponential function (see Materials and Methods) allowed estimation of the buildup rates (k) of the dipolar transfer between the corresponding neighboring carbons. Carbon distances were measured along the double helix (between C2, C3, C5, C6, and C1 and/or C6), but also between helices for C6/C2 and C6/C1 distances, in the B-type packing proposed by Imberty and Perez.[19] Figure 7 illustrates the good agreement obtained between the DARR build up rates and C−C distances drawn from the B-type tridimensional structure. These first results clearly show that determination of internuclear carbon distances is possible by using these different techniques on a highly crystalline labeled sample. However, it seems that the dipolar transfer under DARR is only efficient for distances lower than 0.5 nm. Further work is necessary to check the potentiality of other dipolar recoupling sequences for the determination of longer C−C distances, as for example between carbon atoms belonging to different double helices in the crystal.

Conclusion

This work presents the first high-resolution solid-state NMR spectra of amylose, which were recorded from highly crystalline ^{13}C-labeled axialitic particles. It allows the most complete assignment of the ^{13}C CP-MAS NMR spectra recorded for B-type starch and amylose since the 1990s. Moreover, by using specific sequences, it was possible to determine some carbon−carbon distances in the B-crystal in good agreement with the model existing for this structure. Supplementary sequences would have been necessary to measure distances higher than 0.5 nm. These new experiments open ways to a series of new, exciting experiments especially for assessing the carbon−carbon distances in the other A-type polymorph of starch and amylose, for which a slightly different double helix was proposed, besides a much denser monoclinic packing.[18] It would also be very useful to determine the interactions present in the inclusion complexes of amylose for which only the crystalline packing of amylose single helices is known. The location of the guest molecules cannot have been determined up to now by crystallography.

Acknowledgment. Technical assistance with X-ray diffraction, treatments of the NMR data, and measurements of distances on the B-type structure by B. Pontoire, E. Bellini, and C. Harb, respectively, is gratefully acknowledged by the authors.

References and Notes

(1) Buleon, A.; Colonna, P.; Planchot, V.; Ball, S. *Int. J. Biol. Macromol.* **1998**, *23*, 85−112.
(2) Zobel, H. F. *Starch/Staerke* **1988**, *40*, 44−50.
(3) Gernat, C.; Radosta, S.; Anger, H.; Damashun, G. *Starch/Staerke* **1993**, *45*, 309−314.
(4) Katz, J. R.; Van Itallie, T. B. *Z. Phys. Chem.* **1930**, *A150*, 37.
(5) French, D.; Murphy, V. *Cereal Foods World* **1977**, *22*, 61−70.
(6) Duprat, F.; Galland, D.; Guilbot, A.; Mercier, C.; Robin, J. P. L'amidon. In *Les polymères végétaux*; Monties, B., Ed.; Gauthier-Villars: Paris, 1980.
(7) Sarko, A.; Zugenmaier, P. Amylose and its derivatives. In *Fiber Diffraction Methods*; French, A. D., Gardner, K. H., Eds.; ACS Symposium Series; American Chemical Society: Washington, DC, 1980; pp 459−482.
(8) French, D. Organization of starch granules. In *Starch, chemistry and technology*; Whistler, R. L., Bemiller, J. N., Parschall, E. F., Eds.; Academic Press: New York, 1984; pp 183−247.
(9) Morrison, W. R.; Law, R. V.; Snape, C. C. *J. Cereal Sci.* **1993**, *18*, 107−109.
(10) Buleon, A.; Duprat, A.; Booy, F. P.; Chanzy, H. *Carbohydr. Polym.* **1984**, *4*, 161−173.
(11) Imberty, A.; Chanzy, H.; Perez, S.; Buleon, A.; Tran, V. *Macromolecules* **1987**, *20*, 2634−2636.
(12) Wu, H. C.; Sarko, A. *Carbohydr. Res.* **1978**, *61*, 7−25.
(13) Wu, H. C.; Sarko, A. *Carbohydr. Res.* **1978**, *61*, 26−40.
(14) Ring, S. G.; Miles, M. J.; Morris, V. J.; Turner, R.; Colonna, P. *Int. J. Biol. Macromol.* **1987**, *9*, 158−160.

(15) Pfannemüller, B. *Int. J. Biol. Macromol.* **1987**, *9*, 105−108.
(16) Hizukuri, S. *Agric. Biol. Chem.* **1961**, *25*, 45−49.
(17) Gidley, M. J.; Bulpin, P. V. *Macromolecules* **1989**, *22*, 341−346.
(18) Imberty, A.; Chanzy, H.; Perez, S.; Buleon, A.; Tran, V. *J. Mol. Biol.* **1988**, *201*, 365−378.
(19) Imberty, A.; Perez, S. *Biopolymers* **1988**, *27*, 1205−1221.
(20) Takahashi, Y.; Kumano, T.; Nishikawa, S. *Macromolecules* **2004**, *37*, 6827−6832.
(21) Gidley, M. J.; Bociek, S. M. *J. Am. Chem. Soc*. **1985**, *107*, 7040−7044.
(22) Veregin, R. P.; Fyfe, C. A.; Marchessault, R. H.; Taylor, M. G. *Macromolecules* **1986**, *19*, 1030−1034.
(23) Hewitt, J. M.; Linder, M.; Perez, S.; Buleon, A. *Carbohydr. Res.* **1986**, *154*, 1−13.
(24) Horii, F.; Yamamoto, H.; Hirai, A.; Kitamaru, R. *Carbohydr. Res*. **1987**, *160*, 29−40.
(25) Singh, V.; Ali, S.; Divakar, S. *Starch/Staerke* **1993**, *45*, 59−62.
(26) Morgan, K. R.; Furneaux, R. H.; Larsen, N. G. *Carbohydr. Res*. **1995**, *276*, 387−399.
(27) Paris, M.; Bizot, H.; Emery, J.; Buzare, J. Y.; Buleon, A. *Carbohydr. Polym.* **1999**, *39*, 327−339.
(28) Snape, C. E.; Morrison, W. R.; Maroto-Valer, M. M.; Karkalas, J.; Pethrick, R. A. *Carbohydr. Polym.* **1998**, *36*, 225−237.
(29) Lebail, P.; Buleon, A.; Shiftan, D. R. H.; Marchessault, R. H. *Carbohydr. Polym*. **2000**, *43*, 317−326.
(30) Rondeau-Mouro, C.; Lebail, P.; Buleon, A. *Int. J. Biol. Macromol.* **2004**, *34*, 309−315.
(31) Tanner, S. F.; Ring, S. G.; Whittam, M. A.; Belton, P. S. *Int. J. Biol. Macromol.* **1987**, *9*, 219−224.
(32) Cheetham, N. W. H.; Tao, L. P. *Carbohydr. Polym.* **1998**, *36*, 285−292.
(33) Bogracheva, T. Y.; Wang, Y. L.; Hedley, C. L. *Biopolymers* **2001**, *58*, 247−259.
(34) Lesage, A.; Bardet, M.; Emsley, L. *J. Am. Chem. Soc.* **1999**, *121*, 10987−10993.
(35) Kono, H.; Erata, T.; Takai, M. *Macromolecules* **2003**, *36*, 5131−5138.
(36) Kono, H. *Biopolymers* **2004**, *75*, 255−263.
(37) Kono, H.; Numata, Y.; Erata, T.; Takai, M. *Macromolecules* **2004**, *37*, 5310−5316.
(38) Potocki-Veronese, G.; Putaux, J.-L.; Dupeyre, D.; Albenne, C.; Remaud-Siméon, M.; Monsan, P.; Buléon, A. *Biomacromolecules* **2005**, *6*, 1000−1011.
(39) Potocki de Montalk, G.; Sarçabal, P.; Remaud-Siméon, M.; Willemot, R.-M.; Planchot, V.; Monsan, P. *FEBS Lett.* **2000**, *471*, 219−223.
(40) Potocki de Montalk, G.; Remaud-Siméon, M.; Willemot, R.-M.; Planchot, V.; Monsan, P. *J. Bacteriol.* **1999**, *181*, 375−381.
(41) Wakelin, J. H.; Virgin, H. S.; Crystal, E. *J. Appl. Phys.* **1959**, *30*, 1654−1662.
(42) Marion, D.; Ikura, M.; Tschudin, R.; Bax, A. *J. Magn. Reson.* **1989**, *85*, 393−399.
(43) Duma, L.; Hediger, S.; Lesage, A.; Emsley, L. *J. Magn. Reson*. **2003**, *164*, 187−195.
(44) Takegoshi, K.; Nakamura, S.; Terao, T. *Chem. Phys. Lett.* **2001**, *344*, 631−637.
(45) Andrew, E. R.; Clough, S.; Farnell, L. F.; Gledhill, T. D.; Roberts, I. *Phys. Lett.* **1966**, *21*, 505−506.
(46) Raleigh, D. P.; Levitt, M. H.; Griffin, R. G. *Chem. Phys. Lett.* **1988**, *146*, 71−76.
(47) Levitt, M. H.; Raleigh, D. P.; Creuset, F.; Griffin, R. G. *J. Chem. Phys.* **1990**, *92*, 6347−6364.
(48) Gidley M. J.; Bociek, S. M. *J. Am. Chem. Soc.* **1988**, *110*, 3820−3829.
(49) Veregin, R. P.; Fyfe, C. A.; Marchessault, R. H.; Taylor, M. G. *Carbohydr. Res.* **1987**, *160*, 41−55.
(50) Raleigh, D. P.; Levitt, M. H.; Griffin, R. G. *Chem. Phys. Lett.* **1988**, *146*, 71−76.
(51) Baldus, M. *Prog. Nucl. Magn. Reson. Spectrosc*. **2002**, *41*, 1−47.
(52) Takegoshi, K.; Nakamura, S.; Terao, T. *J. Chem. Phys*. **2003**, *118*, 2325−2341.

BM060330X